

Supporting Information

Microwave-Annealing-Induced Nanowetting of Block Copolymers in Cylindrical Nanopores

Chun-Wei Chang, Ming-Hsiang Cheng, Hao-Wen Ko, Chien-Wei Chu, Yi-Hsuan Tu, and Jiun-Tai Chen

Department of Applied Chemistry, National Chiao Tung University, Hsinchu, Taiwan 30010

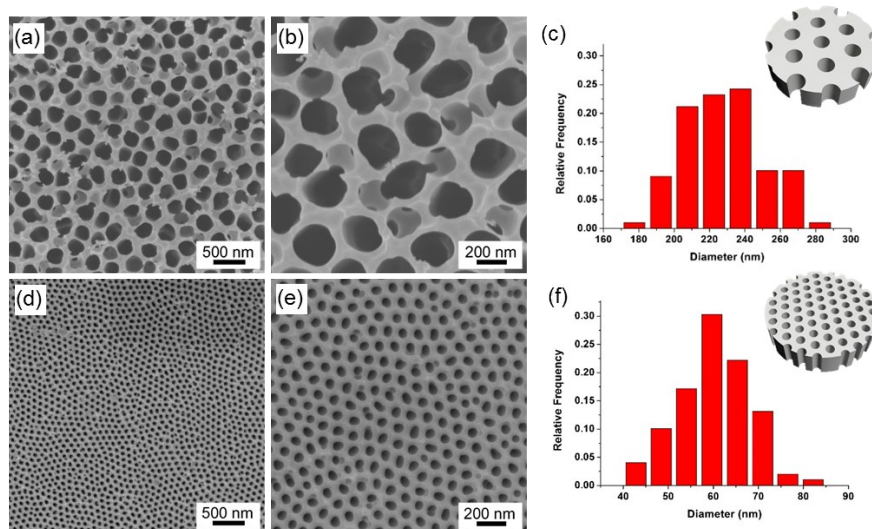


Figure S1. (a and b) SEM images of commercial AAO templates with lower and higher magnifications. (c) Pore size distribution of the commercial AAO templates. The average pore diameter is ~240 nm. An illustration of a commercial AAO template is also included. (d and e) SEM images of synthesized AAO templates with lower and higher magnifications. (f) Pore size distribution of the synthesized AAO templates. The average pore diameter is ~60 nm. An illustration of a synthesized AAO template is also included.

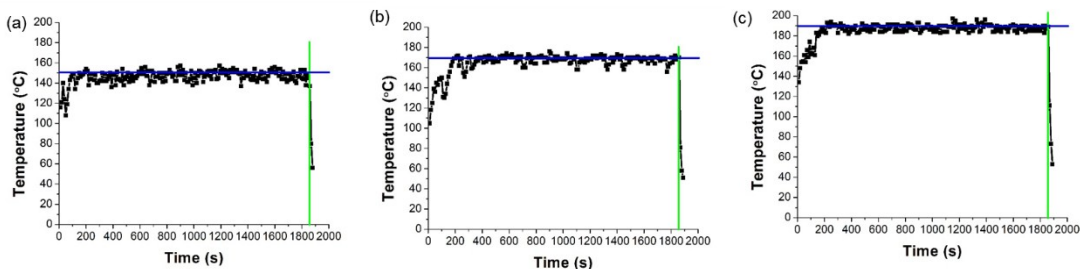


Figure S2. Heating profiles under different microwave annealing conditions using 1×1 cm² silicon wafers: (a) 150 °C at 10 W for 15 min, (b) 170 °C at 15 W for 15 min, and (c) 190 °C at 15 W for 15 min. The blue and green lines indicate the setting annealing temperatures and times, respectively.

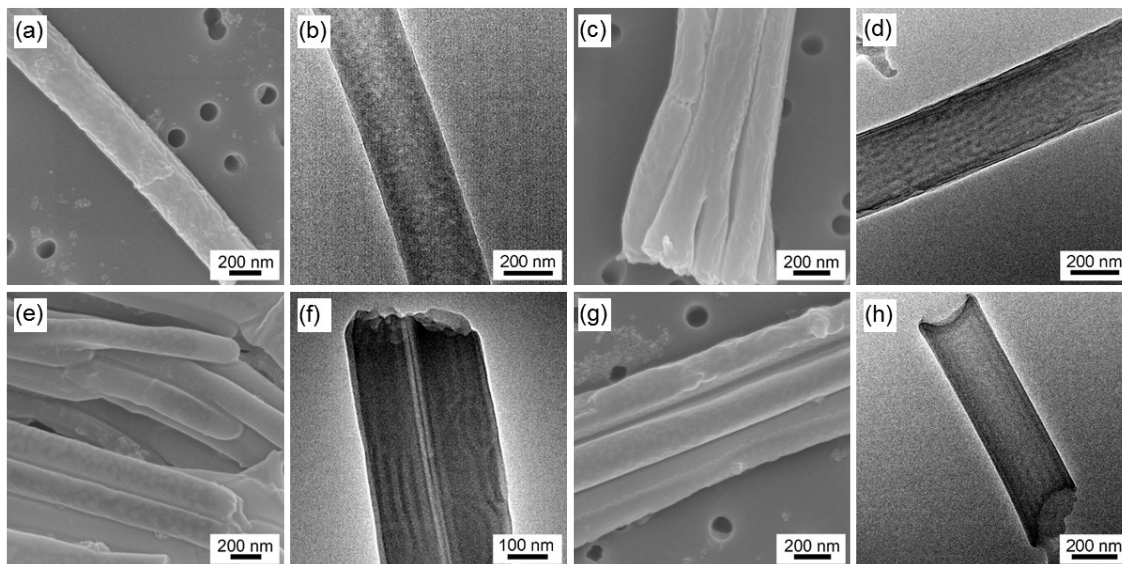


Figure S3. SEM and TEM image of PS-*b*-PDMS nanostructures using the MAIN method with different block copolymer compositions and annealing temperatures: (a and b) PS_{31k}-*b*-PDMS_{14.5k} at 150 °C at 5 W for 15 min, (c and d) PS_{31k}-*b*-PDMS_{14.5k} at 170 °C at 10 W for 15 min, (e and f) PS_{22k}-*b*-PDMS_{21k} at 150 °C at 5 W for 15 min, and (g and h) PS_{22k}-*b*-PDMS_{21k} at 170 °C at 10 W for 15 min.

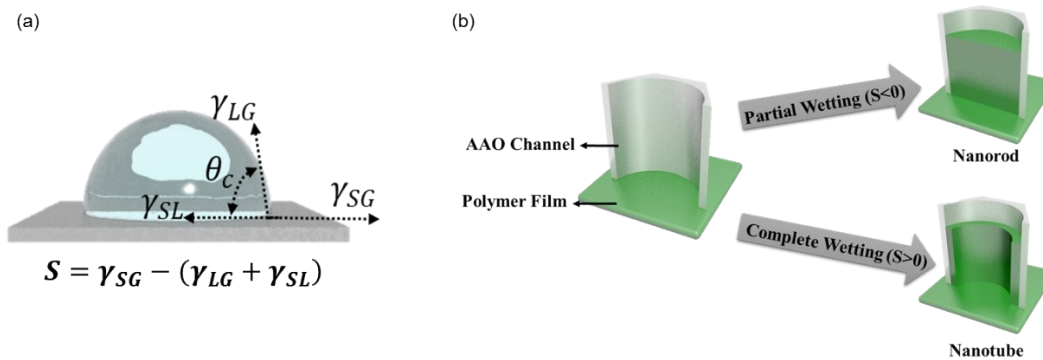


Figure S4. (a) Schematic illustration of the spreading coefficient S , where γ_{SG} is the interfacial tension between the solid and the gas, γ_{LG} is the interfacial tension between the solid and the gas, and γ_{SL} is the interfacial tension between the solid and the liquid. (b) The formation mechanism of nanostructures. Nanotubes are generated when $S > 0$ (complete wetting), and nanorods are generated when $S > 0$ (partial wetting).

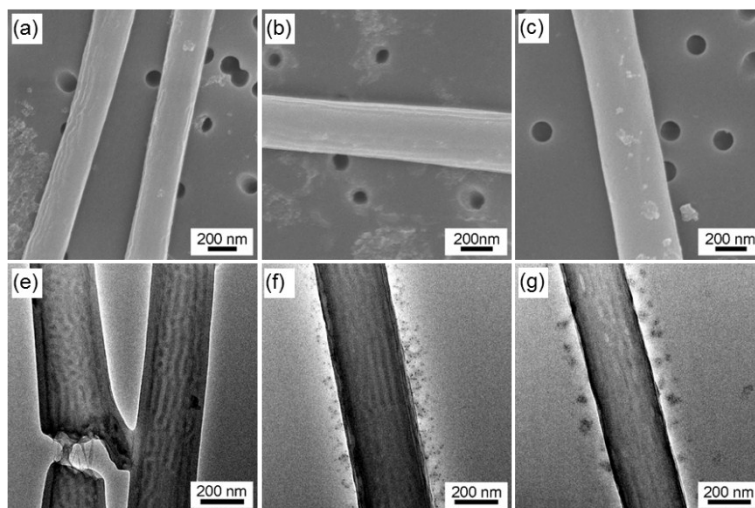


Figure S5. SEM and TEM image of $PS_{31k}\text{-}b\text{-}PDMS_{14.5k}$ nanostructures using the thermal annealing method for 6 h at different annealing temperatures: (a and e) 150 °C, (b and f) 170 °C, and (c and g) 190 °C.

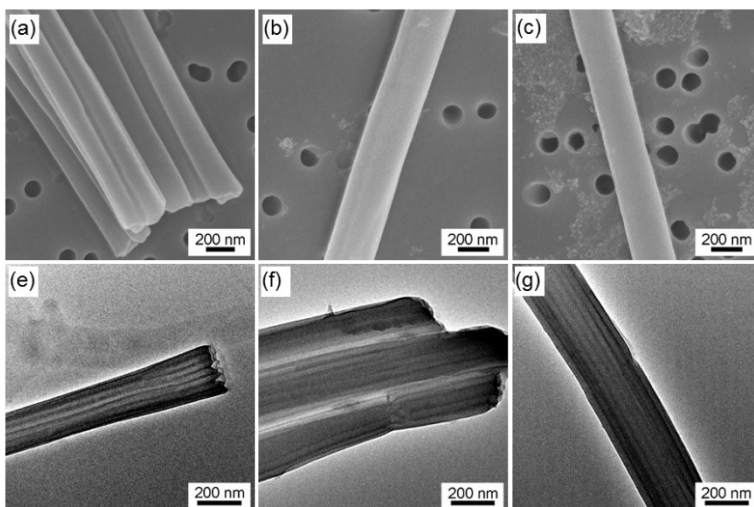


Figure S6. SEM and TEM image of PS_{22k} -*b*- $PDMS_{21k}$ nanostructures using the thermal annealing method for 6 h at different annealing temperatures: (a and e) 150 °C, (b and f) 170 °C, and (c and g) 190 °C.

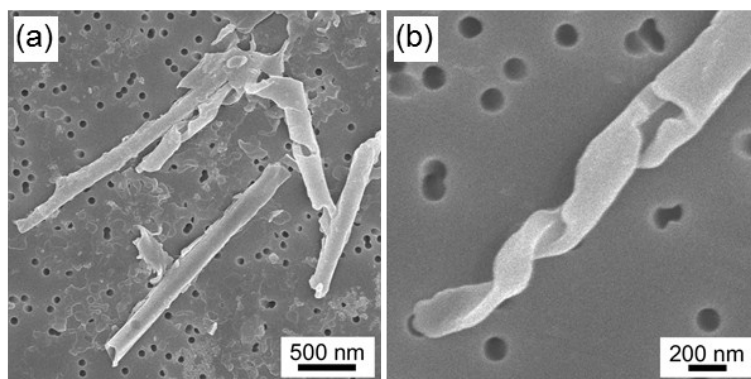


Figure S7. SEM images of PS_{31k} -*b*- $PDMS_{17.5k}$ nanostructures using the thermal annealing method at an annealing temperature of 250 °C for 6 h with lower and higher magnifications.